Published in final edited form as:
Cancer Lett. 2007 May 8; 249(2): 148–156.

The *E705K* mutation in *hPMS2* exerts recessive, not dominant, effects on mismatch repair

Suzanne M. Deschênes[a,*], **Guy Tomer**[b], **Megan Nguyen**[c], **Naz Erdeniz**[c], **Nicole C. Juba**[a], **Natalia Sepúlveda**[a], **Jenna E. Pisani**[a], and **R. Michael Liskay**[c]

a *Department of Biology, Sacred Heart University, 5151 Park Ave., Fairfield, CT 06825, USA*

b *OMRIX Biopharmaceuticals Ltd., Tel Hashomer Hospital, Tel Aviv, Israel*

c *Department of Molecular and Medical Genetics, Oregon Health and Science University, Portland, OR, USA*

Abstract

The *hPMS2* mutation *E705K* is associated with Turcot syndrome. To elucidate the pathogenesis of *hPMS2-E705K*, we modeled this mutation in yeast and characterized its expression and effects on mutation avoidance in mammalian cells. We found that while *hPMS2-E705K* (*pms1-E738K* in yeast) did not significantly affect hPMS2 (Pms1p in yeast) stability or interaction with MLH1, it could not complement the mutator phenotype in MMR-deficient mouse or yeast cells. Further-more, *hPMS2-E705K/pms1-E738K* inhibited MMR in wild-type (WT) mammalian cell extracts or yeast cells only when present in excess amounts relative to WT PMS2. Our results strongly suggest that *hPMS2-E705K* is a recessive loss-of-function allele.

Keywords

Mismatch repair; PMS2; Turcot syndrome

1. Introduction

DNA mismatch repair (MMR) is a highly conserved DNA repair pathway whose primary function is to detect and repair mismatched DNA bases that spontaneously arise during DNA replication and recombination. MMR also participates in the repair of other DNA lesions, acts to suppress recombination between similar but not identical DNA sequences, and plays a role in DNA damage surveillance. Extensive characterization of MMR in bacteria, yeast, and mammals has led to the delineation of two groups of MMR proteins, the MutS and MutL proteins. MutS proteins (e.g., MSH2, MSH6, and MSH3) recognize and bind mismatched or damaged DNA base pairs, while MutL proteins (e.g., MLH1, PMS2, and MLH3) bind MutS proteins and recruit additional proteins for excision of the mismatch and DNA resynthesis (reviewed in [1–6]). In eukaryotes, the primary MutL and MutS complexes are composed of PMS2 (Pms1 in yeast) and MLH1 (MutLα), and MSH2 and MSH6 (MutSα), respectively (reviewed in [1–6]). Defects in the genes coding for these and other MMR proteins result in a

* Corresponding author. Tel.: +1 203 371 7785; fax: +1 203 365 4785. *E-mail address:* descheness@sacredheart.edu (S.M. Deschênes).

mutator phenotype, characterized by higher rates of base pair substitutions and instability in microsatellite sequences (MSI) (reviewed in [1–6]).

The mutator phenotype was associated initially with hereditary nonpolyposis colorectal cancer (HNPCC), a syndrome accounting for ~3% of colorectal cancers and predominantly caused by mutations in *MSH2* and *MLH1*. Until recently, the paucity of germline *PMS2* mutations and the absence of intestinal cancer in *Pms2*$^{-/-}$ mice [7,8] had been widely believed to indicate a minimal role for *PMS2* in the initiation of tumorigenesis, even though ample evidence suggested that PMS2-deficiency results in a mutator phenotype [8–10]. However, recent discoveries of new germline *hPMS2* mutations have significantly reshaped views about the relationship between PMS2 and cancer [reviewed in 11]. Based on their phenotypic effects, germline *hPMS2* defects can now be classified into two groups: (1) compound heterozygosity or homozygosity for recessive *PMS2* mutations is associated with Turcot syndrome and often, café-au-lait spots and childhood onset of hematological cancers [12–16] and (2) heterozygosity for a *PMS2* mutation that is recessive at the cellular level, followed by mutation or loss of the wild-type (WT) allele is associated with classic autosomal dominant inheritance of HNPCC [17–19].

Interestingly, one common feature of kindreds segregating the first group of *PMS2* mutations is that elevated MSI is observed in both tumor and non-neoplastic tissues of the patients, but not in the transmitting parents or in heterozygous family members. The same phenomenon of MSI in normal tissues was described in two reports of Turcot syndrome patients in whom only one *PMS2* mutation was originally detected: R134Ter [20] and E705K [21]. The patients carrying *hPMS2-R134Ter* [20] were later found to carry a recessive mutation in the second *PMS2* allele [14]. This finding, coupled with the lack of MSI in the parents' non-neoplastic tissues and non-dominant functional effects in cultured human cells [22], suggested that *hPMS2-R134Ter* is a recessive allele and not a dominant allele as originally proposed [23]. In this report, we describe the characterization of *hPMS2-E705K* through yeast modeling, expression in mouse cells, and *in vitro* MMR assays. We provide functional evidence that *hPMS2-E705K* is a recessive allele and unlikely to be the sole etiologic factor for Turcot syndrome in this family.

2. Materials and methods

2.1. Yeast strains, vectors, and fluctuation analyses

S. cerevisiae strain W303 (*ade2-1 leu2-3,112 his3-11,15*$_c$ *trp1-1 ura3-1 CAN1 RAD5 hom3-10*; [24]) was used for gene targeting and over-expression studies. Growth conditions for this strain and others generated in this study have been previously described [24], and transformations were performed according to the polyethylene glycol–lithium acetate method [25]. A 446 bp *Aat*II/*Sph*I fragment of pCoB-*yPMS1-E738K* (unpublished) was cloned into *Aat*II/*Sph*I-digested pRS416-*PMS1* [24], generating pRS416-*pms1-E738K*. To generate the 2 μ plasmids pRS426-*PMS1* and pRS426-*pms1-E738K*, *Pvu*II fragments of 4.4 kb from plasmids pRS416-*PMS1* and pRS416-*pms1-E738K* were cloned into *Pvu*II-digested pRS426 [26]. The targeting vector pRS406-*pms1-E738K* was constructed by cloning a 1.5 kb *Spe*I/*Sal*I fragment from pRS416-*pms1-E738K* into *Spe*I/*Sal*I-digested pRS406 [26], and was then linearized with *Hpa*I for integration into the *PMS1* genomic locus of W303 cells by a two-step allele replacement method [27]. Construction of the W303 *pms1*Δ strain was explained previously [24]. Mutations at *hom3-10* and *CAN1* loci in yeast were measured through fluctuation analyses [28], and rates were determined as previously described [29]. The 95% confidence intervals for mutation rates were calculated with PRISM 2.0a software (GraphPad Software, Inc.).

2.2. Cultured cell lines

The spontaneously-immortalized mouse embryonic fibroblast (MEF) cell lines used in this study were: C18 [*Pms2*$^{-/-}$; 30], CAKEM6.7 [WT; 31], MC5 [WT; 8], and MP1 [*Mlh1*$^{-/-}$, *Pms2*$^{-/-}$; 32]. MEF cultures were grown as previously described [33].

2.3. Mammalian expression vectors

The construction of pCPB-hPMS2 has been described previously [33]. The Quikchange site-directed mutagenesis kit (Stratagene) and mutagenesis primers hPMS2E705K.F 5′-CAGCATGCCACGGACAAGAAGTATAACTTCG-3′ and hPMS2E705K.R 5′-CGAAGTTATACTTCTTGTCCGTGGCATGCTG-3′ were used to introduce a G → A mutation in codon 705 of a full-length *hPMS2* cDNA cloned into pBluescript II. The desired point mutation was verified through sequence analysis. *Eco*RI fragments of 2.7 kb in length and containing either the full-length (including a 3′ UTR) WT or mutated *hPMS2* cDNAs were isolated and cloned into the *Eco*RI sites of pCPB to yield the plasmids pCPB-hPMS2 and pCPB-E705K, respectively. The orientations of the cDNA inserts were determined through restriction mapping, and the entire *hPMS2* coding region was sequenced in each plasmid. The construction of the pCNB-hMLH1 vector was described previously [34].

2.4. Transient transfections

Plasmids bearing *hMLH1* and *hPMS2* cDNAs were transiently transfected into MP1 cells in a manner similar to that described previously [33]. Briefly, various combinations and amounts of purified (Endo-free Maxiprep, Qiagen) *hMLH1*, *hPMS2*, *hPMS2-E705K*, pCPB, and pCNB DNAs were introduced into MP1 cells using Lipofectamine and Plus reagents (Invitrogen). The empty vector DNA was used to equalize the mass of DNA transfected in each well of a 6-well plate to a total of 3 μg, and all reactions were performed in duplicate with two different DNA preparations for each construct. Each experiment was repeated 3–4 times.

2.5. Generation of MEF clones stably expressing hPMS2

The C18 cell line was subcloned by limiting dilution, and metaphase spreads of 6 subclones were prepared to identify subclones with diploid DNA content. The diploid subclone C18.2 was expanded and electroporated with 10 μg of pCPB, pCPBhPMS2, or pCPBE705K. Following selection in puromycin for 7 days, 30 clones were expanded in duplicate 12-well plates, and cells from one 12-well plate were subsequently lysed in 1X Laemmli sample buffer.

2.6. Analyses of hPMS2 expression

Whole cell lysates of stably transfected C18.2 clones were electrophoresed on 8% SDS–PAGE gels and transferred to Immobilon-P membrane (Millipore). Immunoblotting was performed using anti-PMS2 monoclonal antibody A16-4 (1:500; BD Pharmingen) which detects both human and mouse PMS2, and anti-MSH6 monoclonal antibody (1:2500 of clone 44; BD Transduction Laboratories) which was used to control for equal loading of samples. Chemiluminescent signals were developed with an enhanced chemiluminescence detection system (Western Lightning, Perkin-Elmer Life Sciences) and captured on Kodak BioMax Light film. The films were imaged on a UVP EC3 Bio-Chemi Imaging System (UVP Corp.), and the absolute integrated optical density of individual protein bands was determined using the Labworks 4.0 software package (UVP Corp.). To control for loading discrepancies, hPMS2 expression was normalized to endogenous mMSH6 expression.

Western analysis of hPMS2 expression in transiently-transfected MP1 cells was performed essentially as described previously [33]. Proteins were detected with primary monoclonal antibodies against hMLH1 (1:200 of clone G168-728; BD Pharmingen), hPMS2 (1:500 of clone A16-4; BD Pharmingen), and α-tubulin (1:1000 of clone B 5-1-2; Sigma). Following

incubation with a 1:5000 dilution of a horseradish peroxidase-coupled goat anti-mouse antibody (Jackson Immunoresearch), ECL Plus Western Blotting Detection Reagents (Amersham) were used to visualize proteins. Chemiluminescent signals were captured with the UVP EC3 BioChemi Imaging System (UVP Corp.), and densitometry was performed as described earlier. PMS2 band densities were divided by the band densities for endogenous mouse α-tubulin in each lane to correct for loading discrepancies.

2.7. MSI analyses

Non-isotopic detection of the frequency of MSI at 5–6 of the mouse dinucleotide repeat loci *D4Mit27*, *D19Mit41*, *D13Mit67*, *D16Mit4*, *D17Mit123*, *and D13Mit139* was performed in up to 12 subclones of each cell line, exactly as described previously [35].

2.8. In vitro MMR assays

The construction of baculovirus expression vectors (pFastBac Dual; Invitrogen) containing full-length *hMLH1* and 6× His tagged-*hPMS2* cDNAs was described previously [32]. To generate a pDUAL-hPMS2-E705K construct, a 1.6 kb *Pvu*II-*Aat*II fragment of the *hPMS2-E705K* cDNA was cloned into the *Pvu*II-*Aat*II sites of the pDUAL-hPMS2 vector and verified through restriction analysis and sequencing of the complete coding region. Recombinant hMutLα was produced in *Spodoptera frugiperda* (Sf9) insect cells using the Bac-to-Bac Baculovirus Expression system (Invitrogen), and purified by nickel affinity and ion exchange chromatography as described previously [32]. The purified proteins were electrophoresed on 8% SDS–PAGE gels, visualized with Coomassie blue stain, and relative amounts were determined with Quantity One software (BioRad).

MP1 and MC2 cell lines were expanded in up to forty 150 mm plates and harvested, and cytoplasmic extracts were prepared as described [36]. The HeLa nuclear extract was a kind gift from Dr. Paul Modrich (Duke Univ. Medical Center, Durham, NC). Circular, double-stranded DNA substrates containing a 5′ nick and either a G/T mismatch or a 1 bp insertion/deletion loop (IDL) were prepared as described earlier [32] and used for *in vitro* MMR assays with the relevant cytoplasmic or nuclear extracts. The percent repair efficiency represents the sum of the intensity (as determined with Quantity One software, BioRad) of repaired DNA substrates divided by the sum of the intensity of repaired and unrepaired DNA substrates.

3. Results

The glutamic acid residue at codon 705 of hPMS2 lies within a highly conserved region of the MLH1-interacting domain of Pms1p in yeast and PMS2 in mice and humans (Fig. 1), suggesting an important functional role for this residue. To elucidate the effects of the *E705K* allele on MMR-mediated mutation avoidance, we used both *in vivo* and *in vitro* methodologies.

3.1. Analyses of mutation rates in yeast expressing pms1-E738K

To determine the effect of the homologous PMS2 mutation *pms1-E738K* on MMR function in yeast, rates of reversion of a +1 T insertion at the *hom3-10* locus [37] were measured in the W303 strain background. Cells with a genomic *pms1-E738K* mutation expressed as much Pms1p as WT cells (data not shown), and exhibited a mutation rate at the *hom3-10* locus comparable to that of a *pms1*δ strain (Table 1). Thus, the *E738K* mutation inactivates MMR but does not appear to affect Pms1p stability in yeast. To determine whether *pms1-E738K* can exert a dominant effect on MMR, WT W303 yeast cells were transformed with either *CEN* (generally single-copy) or 2 μ (high-copy) plasmids bearing *pms1-E738K*, and reverse and forward mutation rates were measured at *hom3-10* and *CAN1* (reports a wide mutational spectrum) loci, respectively. In yeast expressing *pms1-E738K* from a *CEN* plasmid, mutation

rates were low and comparable to that of WT cells expressing either empty plasmid or *PMS1*. In contrast, cells expressing *pms1-E738K* from a 2 μ plasmid exhibited increased mutation rates relative to *PMS1* expressors (Table 1). As *pms1-E738K* exerts dominant effects on MMR in WT cells only when over-expressed, it behaves as a recessive, loss-of-function allele in yeast.

3.2. Expression and functional analyses of WT and mutant hPMS2 in MMR-deficient MEFs

To evaluate the expression of *hPMS2-E705K* in mammalian cells, we used a transient transfection assay that allows rapid assessments of MLH1 and PMS2 stability [33]. As shown in Fig. 2A, hPMS2 and hPMS2-E705K were expressed at nearly equivalent levels in hMutLα-deficient MP1 cells in the presence of hMLH1, which is known to stabilize hPMS2 through direct interaction [33]. To specifically determine whether hPMS2-E705K was less stable than its wild-type counterpart, MP1 cells were transiently-transfected with 0.25–2 μg of *hPMS2* or *hPMS2-E705K* cDNA alone (Fig. 2B). Quantitation of the PMS2 signals on immunoblots revealed that there was no significant difference in stability between WT and mutant hPMS2 in these cells (Fig. 2C).

Next, we tested the ability of *hPMS2-E705K* to complement the mutator phenotype of *Pms2*$^{-/-}$ MEFs (C18 cells). It was expected that hPMS2 would heterodimerize with mMLH1 in MEFs to yield functional MutLα complexes because human and mouse PMS2 are highly conserved and functional transspecies MutLα have been reported previously [34,38]. The mutator phenotypes of a vector-transfected clone and two clones expressing nearly equivalent amounts of WT hPMS2 or hPMS2-E705K (Fig. 3) were analyzed by determining the mutation frequency at 5–6 microsatellite loci. While mutation levels were very low in the WT *hPMS2*-transfected clone, the microsatellite mutation frequencies in vector and *hPMS2-E705K*-transfected cells were comparably elevated (Table 2), indicating that *hPMS2-E705K* cannot complement the mutator phenotype of C18 cells, even when expressed at levels comparable to WT hPMS2.

3.3. Characterization of MMR in MP1 cytoplasmic extracts supplemented with hMutLα-E705K

Our earlier studies had shown that WT but not mutant recombinant hMutLα can complement cytoplasmic extracts of MP1 cells [32]. A similar strategy was used to characterize the mutation avoidance activity of hPMS2-E705K relative to WT PMS2. As shown in Fig. 4A, the amount of hPMS2-E705K is similar to that in both WT hMutLα and a non-functional mutant form of hMutLα (hMutLα-mE34A/pE41A, [32]) with mutations affecting the ATPase activities of both hMLH1 and hPMS2. Thus *E705K* has little, if any, effects on hPMS2 stability. Furthermore, the stoichiometry of MLH1 to PMS2 was comparable in WT and mutant hMutLα complexes, indicating that the mutation has minimal effects on heterodimerization of hMLH1 and hPMS2 in insect cells. Consistent with this conclusion, yeast two-hybrid analysis revealed that Mlh1p:Pms1p-E738K interaction was not significantly reduced relative to WT Mlh1p:Pms1p interaction (data not shown). Taken together, these data suggest that residue 705/738 has minimal effects on hPMS2/Pms1p stability or heterodimerization with hMLH1/Mlh1p.

Next, either hMutLα or hMutLα-E705K was added to cytoplasmic extracts of the MutLα-deficient MEF cell lines MC2 and MP1. MC2 cells are MutLα-deficent because in the absence of MLH1, PMS2 is unstable [e.g., 34]. Whereas hMutLα exhibited efficient 5′ nick-directed repair of a 1 bp IDL, hMutLα-E705K showed little to no activity in repairing the same mismatch, even when present at twice the amount of hMutLα in MC2 extract (Fig. 4B). The same mismatch correction defect was observed in HCT116 (human colorectal carcinoma cells deficient in MLH1) cytoplasmic extracts supplemented with hMutLα-E705K versus hMutLα (data not shown).

To determine if hPMS2-E705K can dominantly inhibit mammalian MMR, purified hMutLα-E705K was added to a HeLa nuclear extract and *in vitro* MMR assays were performed. In this extract endogenous hMutLα is not limiting, as it contains ~100 ng (560 fmol) of endogenous hMutLα, which is twice that required for maximal activity in reconstituted *in vitro* MMR reactions [39]. Thus, we reasoned that only the addition of excess hMutLα (e.g., 200 ng and 400 ng) would be likely to provoke changes in MMR activity. As shown in Fig. 4C, the repair of a 5′ nicked substrate with a G/T mismatch was inhibited by up to 50% when hMutLα-E705K was added. Addition of equivalent amounts of WT hMutLα or hMutLαmE34A/pE41A did not negatively affect MMR in the same extract, excluding the possibility of artifact-induced MMR inhibition (Fig. 4C). Furthermore, the failure of hMutLα-mE34A/pE41A to dominantly inhibit MMR indicates that the mere presence of a non-functional mutant hMutLα complex is not sufficient to explain the negative effects exhibited by hMutLα-E705K. These results are interesting in light of a recent report in which hMutLα was shown to lose single-stranded endonucleolytic activity as a result of either the E705K or mE34A/pE41A substitutions [40]. Finally, the inhibitory effects of excess hMutLα-E705K were also observed for the 5′ nick-directed repair of a 1 bp IDL in HeLa nuclear extract and when defined ratios of purified WT hMutLα and hMutLα-E705K were added to MMR-deficient cytoplasmic extracts (data not shown). Consistent with the results of the yeast mutator assays, then, the *in vitro* MMR data demonstrate that hPMS2-E705K exerted dominant effects on MMR only when present in excess over WT hPMS2.

4. Discussion

In this report, we describe the use of three different model systems to characterize the expression and mutation avoidance function of *hPMS2-E705K*, an allele found in a Turcot syndrome patient [21]. When introduced into yeast, insect, and mouse cells, this mutant Pms1p/hPMS2 was expressed at or near-equivalent levels to its WT counterpart and appeared to heterodimerize with MLH1 with an efficiency comparable to that of WT Pms1p/hPMS2. We demonstrated that the orthologous mutation, *pms1-E738K*, inactivated the mutation avoidance function of MMR in yeast. Similarly, *hPMS2-E705K* did not complement the mutator phenotype of *Pms2*-deficient MEFs. *In vivo*, $Pms2^{-/-}$ MEFs transfected with *hPMS2-E705K* exhibited high microsatellite instability, and *in vitro* purified hMutLα-E705K failed to restore MMR activity in MMR-deficient MEF cytoplasmic extracts. Finally, we found that (1) *pms1-E738K* exerted dominant effects on MMR in WT yeast only when it was over-expressed, and (2) purified hMutLα-E705K could inhibit MMR-proficient HeLa nuclear extracts only when added in excessive amounts. Taken together, our results strongly suggest that *hPMS2-E705K* is a recessive loss-of-function allele rather than a dominant allele.

Assuming that *hPMS2-E705K* is a recessive allele, two alternative explanations for the pathogenesis of Turcot syndrome in the E705K patient [21] can be made. First, a second and possibly different *PMS2* mutation in the patient may have escaped detection because of the confounding effect of paralogous genes on *PMS2* mutation identification [e.g., 14,17] and thus could account for the presence of the phenotype in the E705K patient but not the parents. Indeed, the use of sequencing techniques designed to circumvent *PMS2* pseudogene sequences has led to the identification of compound heterozygosity or homozygosity for recessive *PMS2* mutations in families with no history of colorectal cancer and probands with café-au-lait spots and hematological or brain cancers:, 1221delG/2361delCTTC [12], 1169ins20/1169ins20 [13], R134Ter/2184delTC [14], R802Ter/R802Ter [14,16], and Y181Ter/Y181Ter [16]. These findings, coupled with recent reports of heterozygosity for recessive *PMS2* mutations associated with autosomal dominant inheritance of HNPCC [17–19], suggest that the population frequency of recessive *PMS2* mutations may be as high as the *MSH2* mutant allele frequency, albeit with lower penetrance [18].

Second, the E705K patient may have carried a second recessive, but undetected, mutation in another MMR or DNA repair gene, or in a gene involved in assuring DNA replication fidelity. Heterozygosity for recessive mutations in two different mutation avoidance genes could result in a mutator phenotype through either synergistic effects on mutation rates [41] or “unlinked non-complementation” [42].

Until recently, the significance of the evolutionary conservation of residue 705 and surrounding residues was unknown. After the completion of our studies, Kadyrov and colleagues reported that residue 705 of hPMS2 is critical for a latent, single-stranded endonucleolytic activity in hMutLα that is stimulated in *in vitro* reconstituted MMR reactions [40]. The introduction of the E705K substitution in hPMS2 inactivated the endonucleolytic activity of hMutLα, suggesting that residue 705 is part of a highly conserved amino acid motif in the active site of the latent endonuclease. The same single-stranded endonucleolytic activity has also been observed in yeast MutLα. In this report we extend the above findings by demonstrating that residue 705/738 is critical *in vivo* for the mutation avoidance function of human PMS2 and yeast Pms1p. Thus, the *hPMS2-E705K*-associated inactivation of endonucleolytic activity in hMutLα [40] likely explains the loss-of-function phenotype that we observed in both mammalian and yeast cells.

Acknowledgements

We gratefully acknowledge Sandy Dudley for expert technical assistance, and Dr. Andrew Buermeyer for helpful comments. This work was supported by grants to S.M. Deschênes (NIH F32 CA79200-03; University Research and Creativity Grants, Sacred Heart Univ.), N. Erdeniz (NIH GM045413), G. Tomer (Human Frontier Science Program Fellowship), and R.M. Liskay (NIH GM032741).

References

1. Buermeyer AB, Deschénes SM, Baker SM, Liskay RM. Mammalian DNA mismatch repair. Annu Rev Genet 1999;33:533–564. [PubMed: 10690417]
2. Harfe BD, Jinks-Robertson S. DNA mismatch repair and genetic instability. Annu Rev Genet 2000;34:359–399. [PubMed: 11092832]
3. Schofield MJ, Hsieh P. DNA mismatch repair: molecular mechanisms and biological function. Annu Rev Microbiol 2003;57:579–608. [PubMed: 14527292]
4. Stojic L, Brun R, Jiricny J. Mismatch repair and DNA damage signaling. DNA Repair 2004;3:1091–1101. [PubMed: 15279797]
5. Kunkel TA, Erie DA. DNA mismatch repair. Annu Rev Biochem 2005;74:681–710. [PubMed: 15952900]
6. Iyer RR, Pluciennik A, Burdett V, Modrich PL. DNA mismatch repair: functions and mechanisms. Chem Rev 2006;106:302–323. [PubMed: 16464007]
7. Baker SM, Bronner CE, Zhang L, Plug AW, Robatzek M, Warren G, et al. Male mice defective in the DNA mismatch repair gene *PMS2* exhibit abnormal chromosome synapsis in meiosis. Cell 1995;82:309–319. [PubMed: 7628019]
8. Prolla TA, Baker SM, Harris AC, Tsao JL, Yao X, Bronner CE, et al. *Pmsl* and *Pms2* DNA mismatch repair. Nat Genet 1998;18:276–279. [PubMed: 9500552]
9. Narayanan L, Fritzell JA, Baker SM, Liskay RM, Glazer PM. Elevated levels of mutation in multiple tissues of mice deficient in the DNA mismatch repair gene *Pms2*. Proc Natl Acad Sci USA 1997;94:3122–3127. [PubMed: 9096356]
10. Yao X, Buermever AB, Narayanan L, Tran D, Baker SM, Prolla TA, et al. Different mutator phenotypes in *Mlhl*-versus *Pms2*-deficient mice. Proc Natl Acad Sci USA 1999;96:6850–6855. [PubMed: 10359802]
11. Gryfe R, Gallinger S. Germline *PMS2* mutations: one hit or two? Gastroenterology 2005;128:1506–1509. [PubMed: 15887130]

12. de Rosa M, Fasano C, Panariello L, Scarano MI, Belli G, Iannelli A, et al. Evidence for a recessive inheritance of Turcot's syndrome caused by compound heterozygous mutations within the *PMS2* gene. Oncogene 2000;19:1719–1723. [PubMed: 10763829]
13. Trimbath JD, Petersen GM, Erdman SH, Ferre M, Luce MC, Giardiello FM. Cafe-au-lait spots and early onset colorectal neoplasia (a variant of HNPCC?). Fam Cancer 2001;1:101–105. [PubMed: 14574005]
14. De Vos M, Hayward BE, Picton S, Sheridan E, Bonthron DT. Novel *PMS2* pseudogenes can conceal recessive mutations causing a distinctive childhood cancer syndrome. Am J Hum Genet 2004;74:954–964. [PubMed: 15077197]
15. Agostini M, Tibiletti MG, Lucci-Cordisco E, Chiaravalli A, Morris H, Furlan D, et al. Two *PMS2* mutations in a Turcot syndrome family with small bowel cancers. Am J Gastroenterol 2005;100:1886–1891. [PubMed: 16144131]
16. De Vos M, Hayward BE, Charlton R, Taylor GR, Glaser AW, Picton S, et al. PMS2 mutations in childhood cancer. J Natl Cancer Inst 2006;98:358–361. [PubMed: 16507833]
17. Nakagawa H, Lockman JC, Frankel WL, Hampel H, Steenblock K, Burgart LJ, et al. Mismatch repair gene *PMS2*: disease-causing germline mutations are frequent in patients whose tumors stain negative for PMS2 protein, but paralogous genes obscure mutation detection and interpretation. Cancer Res 2004;64:4721–4727. [PubMed: 15256438]
18. Truninger K, Menigatti M, Luz J, Russell A, Haider R, Gebbers JQ, et al. Immunohistochemical analysis reveals high frequency of PMS2 defects in colorectal cancer. Gastroenterology 2005;128:1160–1171. [PubMed: 15887099]
19. Worthley DL, Walsh MD, Barker M, Ruszkiewicz A, Bennett G, Phillips K, et al. Familial mutations in *PMS2* can cause autosomal dominant hereditary nonpolyposis colorectal cancer. Gastroenterology 2005;128:1431–1436. [PubMed: 15887124]
20. Hamilton SR, Liu B, Parsons RE, Papadopoulos N, Jen J, Powell SM, et al. The molecular basis of Turcot's syndrome. N Engl J Med 1995;332:839–847. [PubMed: 7661930]
21. Miyaki M, Nishio J, Konishi J, Kikuchi-Yanoshita R, Tanaka K, Muraoka M, et al. Drastic instability of tumors and normal tissues in Turcot syndrome. Oncogene 1997;15:2877–2881. [PubMed: 9419979]
22. Yamada NA, Castro A, Farber RA. Variation in the extent of micro satellite instability in human cell lines with defects in different mismatch repair genes. Mutagenesis 2003;18:277–282. [PubMed: 12714694]
23. Nicolaides NC, Littman SJ, Modrich P, Kinzler KW, Vogelstein B. A naturally occurring *hPMS2* mutation can confer a dominant negative mutator phenotype. Mol Cell Biol 1998;18:1635–1641. [PubMed: 9488480]
24. Erdeniz N, Dudley S, Gealv R, Jinks-Robertson S, Liskav RM. Novel PMS1 alleles preferentially affect the repair of primer strand loops during DNA replication. Mol Cell Biol 2005;25:9221–9231. [PubMed: 16227575]
25. Gietz RD, Schiestl RH. Applications of high efficiency lithium acetate transformation of intact yeast cells using single-stranded nucleic acids as carrier. Yeast 1991;7:253–263. [PubMed: 1882550]
26. Sikorski RS, Hieter P. A system of shuttle vectors and yeast host strains designed for efficient manipulation of DNA in *Saccharomyces cerevisiae*. Genetics 1989;122:19–27. [PubMed: 2659436]
27. Scherer S, Davis RW. Replacement of chromosome segments with altered DNA sequences constructed *in vitro*. Proc Natl Acad Sci USA 1979;76:4951–4955. [PubMed: 388424]
28. Tran PT, Liskay RM. Functional studies on the candidate ATPase domains of *Saccharomyces cerevisiae* MutLα. Mol Cell Biol 2000;20:6390–6398. [PubMed: 10938116]
29. Pang Q, Prolla TA, Liskay RM. Functional domains of the *Saccharomyces cerevisiae* Mlhlp and Pmslp DNA mismatch repair proteins and their relevance to human hereditary nonpolyposis colorectal cancer-associated mutations. Mol Cell Biol 1997;17:4465–4473. [PubMed: 9234704]
30. Fritzell JA, Narayanan L, Baker SM, Bronner CE, Andrew SE, Prolla TA, et al. Role of DNA mismatch repair in the cytotoxicity of ionizing radiation. Cancer Res 1997;57:5143–5147. [PubMed: 9371516]
31. Farber RA, Liskay RM. Karvotypic analysis of a near-diploid established mouse cell line Cytogenet. Cell Genet 1974;13:384–396.

32. Tomer G, Buermeyer AB, Nguyen MM, Liskay RM. Contribution of human mlhl and pms2 ATPase activities to DNA mismatch repair. J Biol Chem 2002;277:21801–21809. [PubMed: 11897781]
33. Mohd AB, Palama B, Nelson SE, Tomer G, Nguyen G, Huo X, et al. Truncation of the C-terminus of human MLH1 blocks intracellular stabilization of PMS2 and disrupts DNA mismatch repair. DNA Repair 2006;5:347–361. [PubMed: 16338176]
34. Buermever AB, Wilson-Van Patten C, Baker SM, Liskav RM. The human *MLH1* cDNA complements DNA mismatch repair defects in *Mlh1*-deficient mouse embryonic fibroblasts. Cancer Res 1999;59:538–541. [PubMed: 9973196]
35. Gurtu VE, Verma S, Grossmann AH, Liskay RM, Skarnes WC, Baker SM. Maternal effect for DNA mismatch repair in the mouse. Genetics 2002;160:271–277. [PubMed: 11805062]
36. Thomas DC, Umar A, Kunkel TA. Measurement of heteroduplex repair in human cell extracts. Methods: Companion Methods Enzymol 1995;7:187–197.
37. Chen C, Merrill BJ, Lau PJ, Holm C, Kolodner RD. *Saccharomyces cerevisiae pol30* (proliferating cell nuclear antigen) mutations impair replication fidelity and mismatch repair. Mol Cell Biol 1999;19:7801–7815. [PubMed: 10523669]
38. Wu X, Platt JL, Cascalho M. Dimerization of MLH1 and PMS2 limits nuclear localization of MutLa. Mol Cell Biol 2003;23:3320–3328. [PubMed: 12697830]
39. Dzantiev L, Constantin N, Genschel J, Iyer RR, Burgers PM, Modrich P. A defined human system that supports bidirectional mismatch-provoked excision. Mol Cell 2004;15:31–41. [PubMed: 15225546]
40. Kadyrov FA, Dzantiev L, Constantin N, Modrich P. Endonucleolytic function of MutLa in human mismatch repair. Cell 2006;126:297–308. [PubMed: 16873062]
41. Drotschmann K, Clark AB, Tran HT, Resnick MA, Gordenin DA, Kunkel TA. Mutator phenotypes of yeast strains heterozygous for mutations in the *MSH2* gene. Proc Natl Acad Sci USA 1999;96:2970–2975. [PubMed: 10077621]
42. Stearns T, Botstein D. Unlinked noncomplementation: isolation of new conditional-lethal mutations in each of the tubulin genes of *Saccharomvces cereyisiae*. Genetics 1988;119:249–260. [PubMed: 3294100]

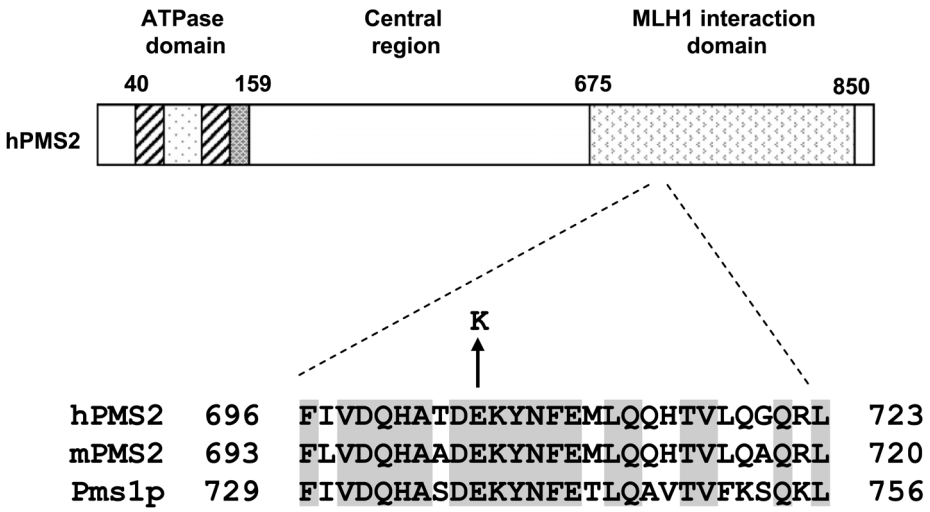

Fig. 1.

Conservation of residue E705 in PMS2 homologs. The non-conservative E → K substitution occurs in hPMS2 residue 705, which is located in a highly conserved region of the MLH1 interaction domain.

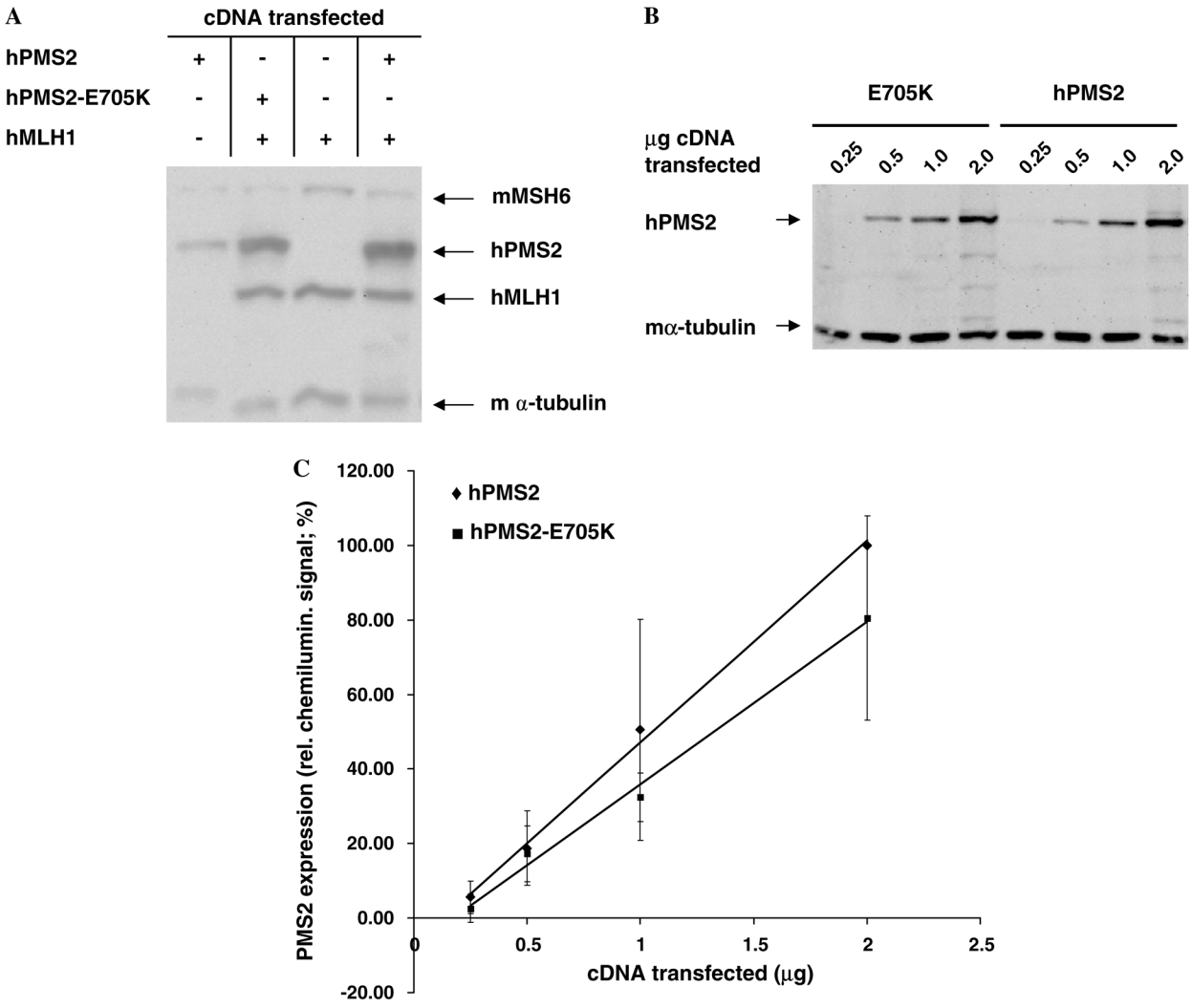

Fig. 2.

Expression of *hPMS2-E705K* in transiently transfected mouse cells. (A) Representative immunoblot of whole cell lysates (WCLs) of MP1 cells transfected with *hMLH1* (1 μg). *hPMS2* (0.25 μg,), and/or *hPMS2-E705K* (0.25 μg) cDNAs, together with pCPB (1.25–1.5 μg) and pCNB (0.5–1.5 μg) empty vector DNAs to bring the total amount of DNA transfected to 3 μg. (B) Representative immunoblot of WCLs of MP1 cells transfected with 0.25–2 μg of *hPMS2* or *hPMS2-E705K* cDNAs. (C) Quantitative analysis of PMS2 expression in MP1 cells transfected with increasing amounts of *hPMS2* versus *hPMS2-E705K* cDNAs. Each point on the graph represents the average of 3–4 experiments consisting of duplicate transfections. Linear regression was performed on each data series.

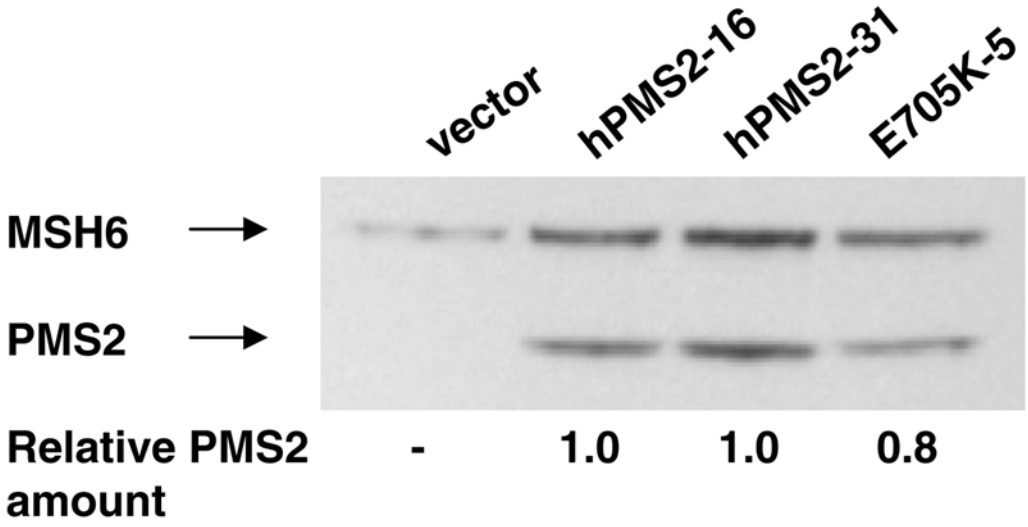

Fig. 3.

Expression of hPMS2 and hPMS2-E705K in stably transfected mouse cells. Whole cell lysates prepared from a subset of C18.2 clones expressing nearly equivalent amounts of hPMS2 and hPMS2-E705K were electrophoresed, immunoblotted, and quantitated via densitometry as described in Section 2. All PMS2 signals were normalized to endogenous mMSH6 expression in each lane, and relative amounts of PMS2 were calculated by dividing all PMS2 signals by the signal detected in clone hPMS2-16 (lane 2).

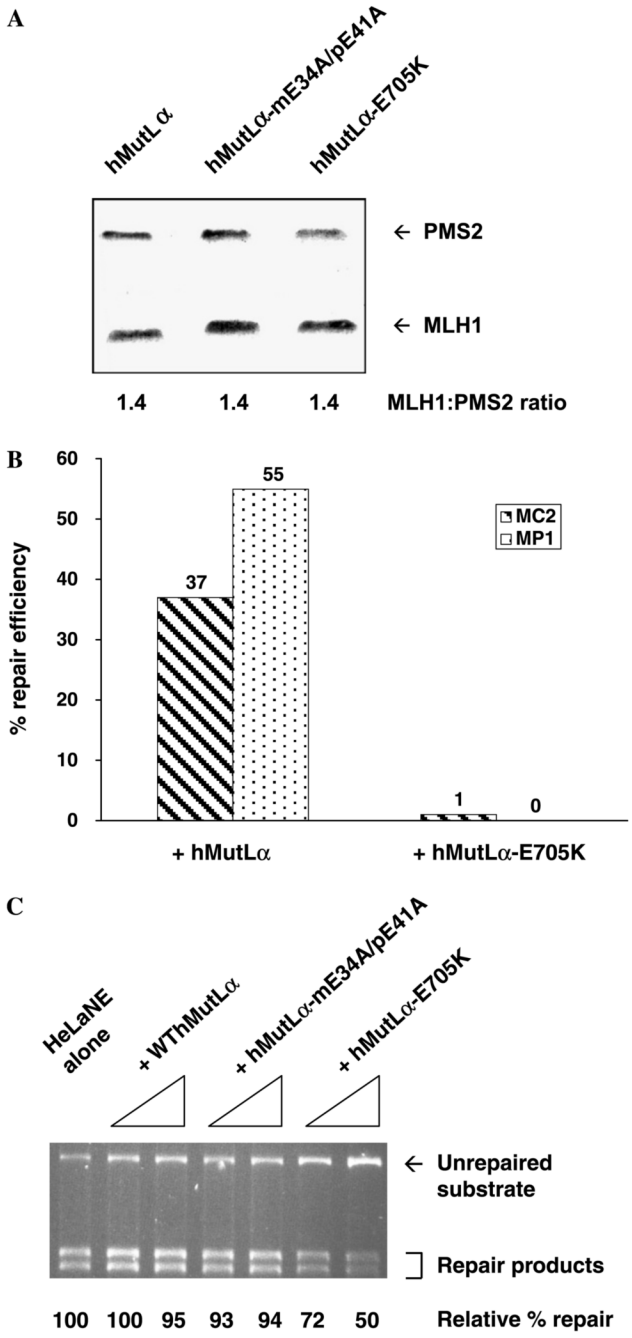

Fig. 4.

In vitro analyses of the ability of hMutLα-E705K to complement MMR deficiency or dominantly inhibit MMR.(A) Coomassie-stained SDS–PAGE gel containing recombinant wild-type and mutant hMutLα that was purified from baculovirus-transduced insect cells through nickel affinity and ion exchange chromatography. hMutLα-mE34A/pE41A, a non-functional hMutLα complex with wild-type MLH1/PMS2 stoichiometry [31], was included for comparison purposes. (B) The 5′ nick-directed repair of a 1 bp IDL was determined in cytoplasmic extracts of MutLa-deficient MEFs supplemented as follows: 350 ng of wild-type or 700 ng of mutant MutLα was added to MC2 extract, whereas 100 ng of either complex was added to MP1 extract. (C) To a HeLa nuclear extract, 200–400 ng of wild-type or mutant

hMutLα was added and its ability to perform 5′ nick-directed repair of a G/T mismatch was determined through agarose gel electrophoresis and densitometry.

Table 1

Effects of genomic and plasmid-borne *pms1-E738K* mutations on mutation rates in the W303 strain of *S. cerevisiae*

Genotype (genome)	*hom3-10*		Genotype(plasmid)[a]	*hom3-10*		*CAN1*	
	Mutation rate ($\times 10^{-8}$)	Fold increase		Mutation rate ($\times 10^{-8}$)[a,b]	Fold increase	Mutation rate ($\times 10^{-8}$)[a,b]	Fold increase
PMS1	1.4	1	Empty vector	0.9 (0.7–1.1)	1	24 (11–37)	1
*pms1*Δ	873	642	*PMS1 (CEN)*	1.1 (0.6–1.6)	1.2	30 (23–37)	1.3
pms1-E738K	971	714	*pms1-738 (CEN)*	1.7 (0.9–2.5)	1.9	36 (18–53)	1.5
			PMS1 (2 μ)	3.3 (1.4–5.2)	3.7	27 (23–30)	1.1
			pms1-738 (2 μ)	213 (165–262)	237	184 (54–314)	7.7

[a] In WT W303 yeast cells.

[b] 95% confidence intervals are indicated in parentheses.

Table 2

Frequency of MSI in *Pms2*-deficient MEFs stably transfected with *hPMS2* or *hPMS2-E705K*

Cell line	MSI frequency (%)
Vector	13.3
hPMS2-31	4.6
E705K-5	18.3